

# PROBING THE STATISTICS OF THE TEMPERATURE-DENSITY RELATION OF THE INTERGALACTIC MEDIUM

TAOTAO FANG<sup>1</sup> AND MARTIN WHITE

Department of Astronomy, University of California, 601 Campbell Hall, Berkeley, CA 94720

Received 2003 December 10; accepted 2004 March 11; published 2004 April 5

## ABSTRACT

Gravitational instability induces a simple correlation between the large- and small-scale fluctuations of the Ly $\alpha$  flux spectrum. However, nongravitational processes involved in structure formation and evolution will alter such a correlation. In this Letter, we explore how scatter in the temperature-density relation of the intergalactic medium reduces the gravitationally induced scale-scale correlation. By examining whether or not observations of the correlation are close to that predicted by pure gravity, we put constraints on the scatter in the  $\rho$ - $T$  relation and in turn on any physical process that would lead to scatter, e.g., strong fluctuations in the UV background or radiative transfer effects. By applying this method to high-resolution Keck spectra of Q1422+231 and HS 1946+7658, we find the predicted correlation signal induced by gravity and the diminishing of this correlation signal at small scales. This suggests extra physics affects the small-scale structure of the forest, and we can constrain the scatter in the  $\rho$ - $T$  relation to a conservative 20% upper limit. A crude model suggests, if there is any spatial correlation of temperature, the coherence length scale must be smaller than  $\sim 0.3 h^{-1}$  Mpc to be consistent with the Keck data.

*Subject headings:* cosmology: theory — intergalactic medium — large-scale structure of universe — methods: numerical — methods: statistical

## 1. INTRODUCTION

In the last few years, our understanding of small-scale structure at high redshift has increased enormously through the study of the Ly $\alpha$  forest, the series of absorption features in the spectra of distant QSOs. Based in large part on insights gained from numerical simulations (see, e.g., Cen et al. 1994; Zhang, Aninos, & Norman 1995; Hernquist et al. 1996), we now know that the physics governing the Ly $\alpha$  forest is relatively simple. At the relevant redshifts, the gas making up the intergalactic medium (IGM) is in photoionization equilibrium, which results in a tight density-temperature relation for the absorbing material with the neutral hydrogen density proportional to a power of the baryon density. Since pressure forces are subdominant, the neutral hydrogen density closely traces the total matter density on the scales relevant to the forest ( $0.1$ – $10 h^{-1}$  Mpc). The structure in QSO absorption thus traces, in a calculable way, slight fluctuations in the matter density of the universe back along the line of sight to the QSO, with most of the Ly $\alpha$  forest arising from overdensities of a few times the mean density (see, e.g., Croft et al. 1998, 2002).

While most attention has focused on the low-order statistics of the Ly $\alpha$  forest, the statistical properties of the flux are significantly non-Gaussian. Viel et al. (2004) studied the bispectrum of a large sample of the QSO Ly $\alpha$  flux spectrum. While their results from observations and simulations and theoretical predictions reasonably agree with each other at large scales, they found the errors on the bispectrum are too large to discriminate between models with different Ly $\alpha$  forest distribution based on the bispectrum method.

However, while in general probing high- $z$  physics with the bispectrum is complicated, in some special cases patterns of higher order correlations can be visible in the moments of the flux. One particular pattern is that due to the action of gravity in hierarchical structure formation. The presence or absence of this pattern provides us with a powerful probe of “extra” physical effects, beyond gravity, in the formation of the Ly $\alpha$  forest, as first emphasized by Zaldarriaga, Seljak, & Hui (2001, here-

after ZSH01). These authors noted that it was possible to constrain fluctuations in the continuum by appealing to higher order moments of the flux. In this Letter, we wish to address another physical effect: scatter in the density-temperature relation induced, for example, by different thermodynamical histories for the gas, fluctuations in the UV background radiation field, or radiative transfer effects. We shall see that it is possible to put tight constraints on the scatter in the  $\rho$ - $T$  relation by considering the higher order moments of the spectra.

The outline of this Letter is as follows. In § 2, we briefly discuss the simulations involved in this work and how we extract “mock” Ly $\alpha$  spectra. The statistical method introduced by ZSH01 is reviewed in § 3. Our main results are presented in § 4, and we discuss the application to high-resolution Keck spectra in § 5. In § 6, we discuss several related issues.

## 2. SIMULATION

Since we are interested in the higher order correlations in the Ly $\alpha$  flux that are induced by gravitational processes, we first need a model of gravitational clustering. For this purpose, we use a particle mesh (PM) code to follow the evolution of dark matter clustering, including only gravity. Details of the PM simulation can be found in Meiksin, White, & Peacock (1999), White (1999), and Meiksin & White (2003). Given the particles’ positions and velocities, the Ly $\alpha$  forest spectrum can be constructed based on the so-called fluctuating Gunn-Peterson approximation, in which Ly $\alpha$  absorbing gas is assumed to trace the dark matter distribution and be in a state of photoionization equilibrium with the UV background radiation (see, e.g., Cen et al. 1994; Zhang et al. 1995; Hernquist et al. 1996; Hui & Gnedin 1997). Under these assumptions, the gas temperature can be obtained through

$$T = T_0 \left( \frac{\rho}{\bar{\rho}} \right)^{\gamma-1}, \quad (1)$$

where  $\rho$  is the matter density and  $\bar{\rho}$  the cosmic mean. The index  $\gamma$  is expected to vary from near unity right after reionization

<sup>1</sup> Chandra Fellow.

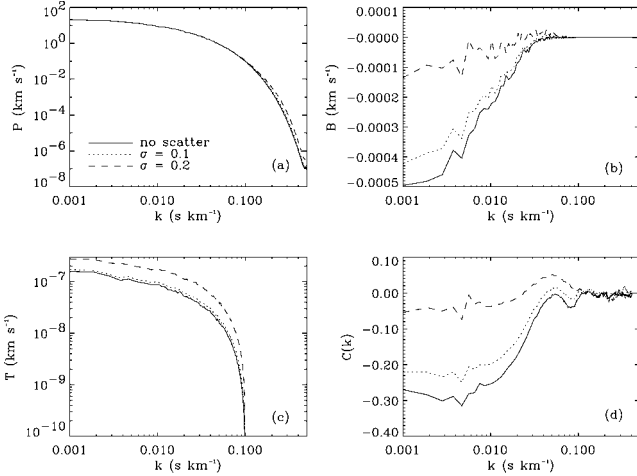


FIG. 1.—Statistics of the Ly $\alpha$  flux spectrum based on a square filter  $0.2 \text{ s km}^{-1} \leq k \leq 0.3 \text{ s km}^{-1}$ . Solid lines show the no-scatter case, dashed lines  $\sigma = 0.1$ , and dotted lines  $\sigma = 0.2$ . (a) Power spectrum. (b) Bispectrum. (c) Trispectrum. (d) Cross-correlation coefficient  $C(k)$ . In (d),  $C(k)$  is smoothed with a boxcar method for visual clarity.

to  $\sim 1.5$  at low  $z$  (Hui & Gnedin 1997). We will set  $T_0 = 2 \times 10^4 \text{ K}$  throughout, but in § 3 we will introduce scatter around the values given by equation (1).

The neutral hydrogen number density, based on our ionization equilibrium assumption, is  $n_{\text{HI}} \propto (\rho/\bar{\rho})^2 T^{-0.7}$ , with the constant of proportionality dependent on the baryon density, redshift, and hydrogen photoionization rate. We shall fix it using the observed value of the mean flux (see below). With the gas density, temperature, and velocity data, the optical depth  $\tau$ , at a given velocity  $u$  is

$$\tau = \int n_{\text{HI}}(x) \sigma(x) dx \propto \int dx \left( \frac{\rho}{\bar{\rho}} \right)^2 T^{-0.7} b^{-1} \exp \left[ -\frac{(u - u_0)^2}{b^2} \right], \quad (2)$$

where  $u_0$  is the sum of Hubble expansion and peculiar velocity at position  $x$ , and  $b = (2k_B T/m_p)^{1/2}$  is the Doppler parameter. Here  $m_p$  is the proton mass, and  $\sigma$  is the photoionization cross section. The flux at velocity  $u$  is then  $\exp(-\tau)$ .

For definiteness, we concentrate on the  $z = 3$  output of a  $512^3$  particle and  $1024^3$  mesh PM simulation in a box of side  $60 h^{-1} \text{ Mpc}$ , which gives a simulation resolution of  $\sim 6 \text{ km s}^{-1}$  at  $z \sim 3$ . The cosmology simulated was of the  $\Lambda\text{CDM}$  family, with  $\Omega_{\text{mat}} = 0.3$ ,  $h = 0.67$ , and  $\sigma_8 = 0.9$ . The density and velocity fields were Gaussian smoothed by  $100 h^{-1} \text{ kpc}$  to simulate the effects of gas pressure, and  $32^2$  spectra, each of  $1024$  pixels, were computed on a regular grid parallel to the box axes. The normalization constant was fixed to reproduce the mean flux,  $\bar{F} = 0.684$ , observed by McDonald et al. (2000) at  $z = 3$  (see also Appendix B of Meiksin & White 2004).

### 3. STATISTICS

To constrain scatter in the temperature-density relationship on small scales, we adopt the high-order statistical method proposed by ZSH01. We briefly describe this technique here and refer the reader to their paper and Mandelbaum et al. (2003) for details.

We define the relative fluctuation of the flux,  $\delta_F \equiv F/\bar{F} - 1$ , and its Fourier transform

$$F(k) = \int dx e^{ikx} \delta_F(x). \quad (3)$$

We bandpass filter  $\delta_F$  with a window function  $W(k)$ :  $F_f(k) = F(k)W(k)$ , taking the window function  $W(k)$  to be either a square window,

$$W_{k_1, k_2}(k) = \begin{cases} 1 & \text{if } k_1 \leq k \leq k_2, \\ 0 & \text{otherwise,} \end{cases} \quad (4)$$

or a Gaussian window function. Our results are not sensitive to this choice, so in what follows we shall concentrate on the square window.

The filtered field  $F_f(k)$  in Fourier space is then inverse transformed back into real space to define

$$\delta_H(x) = \int \frac{dk}{2\pi} e^{-ikx} F_f(k), \quad (5)$$

and this is squared to produce  $h(x) \equiv \delta_H^2(x)$ . Following the conventions in Mandelbaum et al. (2003), we define  $P$  as the power spectrum of  $\delta_F$ ,  $T$  as the power spectrum of  $h$ , and  $B$  as the cross-spectrum between  $\delta_F$  and  $h$ . Since  $h$  depends quadratically on  $\delta_F$ ,  $B$  and  $T$  can be related to the flux bispectrum and trispectrum, respectively. We also introduce the same cross-correlation coefficient  $C(k)$  to study the effect of large-scale density fluctuation on small-scale power, defining  $C \equiv B/\sqrt{PT}$ .

### 4. SCATTER IN $\rho$ - $T$

We model the scatter in the temperature-density relation as lognormal in  $T$  at fixed  $\rho$ , with mean value determined from equation (1). We choose the width,  $\sigma$ , to mimic the results seen in hydrodynamic simulations. Specifically, we choose  $\sigma \equiv \delta \ln T = 0.1$  and  $\sigma = 0.2$  to study the effect. For comparison, by checking the  $\rho$ - $T$  scatter plot, we find a scatter of  $\sigma = 0.1$  ( $0.2$ ) is consistent with results from low- (high-)resolution hydrodynamic simulations in Bryan et al. (1999), respectively (see their Fig. 3). Figure 1a shows the power spectrum  $P$  of our simulation under the assumptions of no scatter,  $\sigma = 0.1$ , or  $\sigma = 0.2$ . At  $k \gtrsim 0.1 \text{ s km}^{-1}$  (scales  $\lesssim 10 h^{-1} \text{ Mpc}$ ), scatter in the temperature-density relation adds power.

We show in Figure 1 the power spectrum, bispectrum, trispectrum, and cross-correlation coefficient from the simulations with a top-hat filter with modes of  $0.2 \text{ s km}^{-1} \leq k \leq 0.3 \text{ s km}^{-1}$ . We chose that range to maximize the effect of  $\rho$ - $T$  scatter on  $C(k)$ . As pointed out by ZSH01, a positive correlation between the large-scale density fluctuations and the power on small scales is induced by gravitational instability. Since, within the “fluctuating Gunn-Peterson approximation,” the fluctuations in the dark matter distribution are directly traced by fluctuations in the Ly $\alpha$  forest, the positive correlation induced by gravitational instability is manifest in the Ly $\alpha$  flux. In the Ly $\alpha$  forest, the correlation is negative since the flux decreases with increasing density.

We see that our model for scatter in the  $\rho$ - $T$  relation does not change the large-scale fluctuations of the Ly $\alpha$  flux spectrum; however, by locally varying the optical depth  $\tau$  through equation (2), it effectively adds noise at small scales. Figure 1d shows

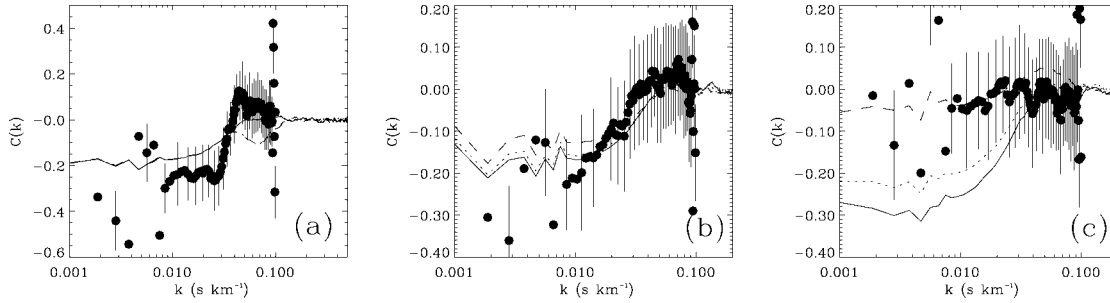


FIG. 2.—Cross-correlation coefficient,  $C(k)$ , for different filtering schemes. Symbols are the same as those in Fig. 1. (a)  $0.02 \text{ s km}^{-1} \leq k \leq 0.06 \text{ s km}^{-1}$ . (b)  $0.1 \text{ s km}^{-1} \leq k \leq 0.2 \text{ s km}^{-1}$ . (c)  $0.2 \text{ s km}^{-1} \leq k \leq 0.3 \text{ s km}^{-1}$ . Keck data are plotted as filled circles. Error bars are  $1 \sigma$  and plotted every three points for visual clarity.

$C(k)$  at low  $k$  becomes steadily less negative as the scatter is increased. Note also that the bispectrum, trispectrum, and cross-correlation coefficient go quickly to zero for  $k \geq 0.1 \text{ s km}^{-1}$ . This is because after filtering the highest mode in the squared field,  $h(k)$ , is  $k_2 - k_1$ , or  $0.1 \text{ s km}^{-1}$  in this case.

Finally, we have investigated the requirements on signal-to-noise ratio (S/N) and resolution of spectra that would be suitable for measuring  $C(k)$  on the appropriate scales. By adding Gaussian random pixel noise to our mock spectra, we found that an S/N approaching 50–100 is required in order not to wash out the small-scale signal. We also notice that the level of scatter is closely related to the simulation resolution. The flux spectrum is obtained by averaging out fluctuations in simulation cells over the thermal broadening width. The smaller the cells are, the more cells will be averaged out, and the smaller the fluctuation will be. In our simulation, the typical temperature of the IGM is  $\sim 2 \times 10^4 \text{ K}$ , which corresponds to a size of  $\sim 18 \text{ km s}^{-1}$ . So the flux spectrum in each pixel is roughly averaged over three neighboring cells. To test this effect, we check simulations with two other resolutions that are close to the ones in hydrodynamic simulations by Bryan et al. (1999), which are 2 and 4 times higher than the one used in the paper. We found that there are no significant differences among these cases.

## 5. AN APPLICATION TO QUASAR DATA

In this section, we study the cross-correlation coefficient  $C(k)$  with two high-resolution, high-S/N quasar spectra, Q1422+231 at  $z = 3.62$  (Rauch et al. 2001) and HS 1946+7658 at  $z = 3.05$  (Kirkman & Tytler 1997). These two quasars were observed with the Keck High Resolution Echelle Spectrometer, with an S/N of  $\sim 140$  and  $\sim 50$ – $100$ , respectively. We split the two spectra into a total of 13 separate pieces between Ly $\alpha$  and Ly $\beta$  emission to avoid contamination from Ly $\beta$  absorption. Each piece has a comoving length of  $60 h^{-1} \text{ Mpc}$  to match our PM simulation. We calculate  $C(k)$  among these 13 samples following the method described in § 3 and compare these results against our PM simulation. We made no attempt to correct for metal lines. In order to account for evolution in the mean flux, we adjusted each spectral segment to  $\langle F \rangle = 0.684$  by scaling the implied optical depths as in the simulations.

In Figure 2, we show  $C(k)$  from both Keck data and our PM simulation. To study the filter effect, we select three filters: (a)  $0.02 \text{ s km}^{-1} \leq k \leq 0.06 \text{ s km}^{-1}$ , (b)  $0.1 \text{ s km}^{-1} \leq k \leq 0.2 \text{ s km}^{-1}$ , and (c)  $0.2 \text{ s km}^{-1} \leq k \leq 0.3 \text{ s km}^{-1}$ . With each filter, we plot the no-scatter case (solid lines), scattering with  $\sigma = 0.1$  (dotted lines), and scattering with  $\sigma = 0.2$  (dashed lines).

Keck data are labeled as filled circles, with error bars computed from the simulations (the sample size in the data is too small to give constraints on variances).

Clearly, with large fluctuations, negative signals are present in cases with filters *a* and *b*, which agrees with the simulation quite well. This is consistent with what ZSH01 found in Q1422+231 data and confirms the correlation between the large- and small-scale fluctuations of the Ly $\alpha$  flux spectrum induced by gravitational instability. Also in cases *a* and *b*, there is almost no difference between no-scatter and scatter because their power spectra (see Fig. 1a) show no difference between  $0.01$  and  $0.2 \text{ s km}^{-1}$ . At smaller scales (larger  $k$ -modes), the scattering increases the power spectrum and starts to differentiate between the scatter and no-scatter cases. We also find, with filter *c*, the  $C(k)$  from Keck data is essentially zero, consistent with 20% scatter in the  $\rho$ - $T$  relation case. Although other effects (such as random noise) may also drive  $C(k)$  to zero, increasing the  $\rho$ - $T$  scatter above 20% drives  $C(k)$  positive, so we can conservatively set an upper limit of 20% on the scatter in the  $\rho$ - $T$  relation.

In the above, we adopted an independent random Gaussian-distributed  $T$  for each pixel. In reality, however, pixels tend to correlate with neighbor pixels: pixels around a high- $T$  pixel appear to also have a high temperature and vice versa. Such a correlation among pixels tends to produce a “correlated” noise from  $\rho$ - $T$  scatter and enhance the signals in cross-correlation coefficient  $C(k)$ : the larger the correlated pixel length scale, the stronger the  $C(k)$ . So with filter *c*, we can ask: What is the largest length scale at which pixels can be correlated with each other, without showing a strong signal in  $C(k)$ , that conflicts with the Keck data? We can parameterize this by adopting a correlation parameter  $r$ :  $T_i = rT_{i-1} + (1-r)T_{\text{new}}$ , where  $T_i$  is the temperature of pixel  $i$ ,  $T_{\text{new}}$  is the temperature obtained from an independent random draw, and  $r$  is a number between 0 and 1;  $r = 0$  means pixels are independent of each other, while  $r = 1$  is the maximum correlation. We found, for the 20% scatter case,  $r$  must be smaller than  $\sim 0.3$ – $0.5$  to be not ruled out by the Keck data. This roughly corresponds to a distance of  $\sim 5$  pixels if we define 2 pixels correlated at the 1% level as “correlated.” This means, with a 20% scatter, the correlated scale length must be smaller than  $\sim 0.3 h^{-1} \text{ Mpc}$ , or  $\sim 30 \text{ km s}^{-1}$ .

The observational evidence for the gravitationally induced correlation, and for small-scale decorrelation, currently rests on two high-resolution spectra. It would obviously be of some interest to improve the analysis presented here and to increase the sample of QSO spectra for which the analysis has been performed.

## 6. DISCUSSION

ZSH01 showed that gravitational instability, and the assumption of the fluctuating Gunn-Peterson approximation, predict a specific correlation between large- and small-scale power in the Ly $\alpha$  forest. They also showed, based on high-resolution Keck data, that observations were consistent with the correlation predicted by gravity. Here we point out that this observation allows one to limit the deviations from the fluctuating Gunn-Peterson approximation and in particular to constrain the fluctuations in the density-temperature relation of the IGM. Such fluctuations are expected to arise from varying thermodynamical histories for the gas and from fluctuations in the ultraviolet background radiation field or radiative transfer effects. We find that these fluctuations must be  $\lesssim 20\%$  in  $T$  at fixed  $\rho$  in order to be consistent with high-resolution Keck data.

Our method provides a sensitive way to probe for scatter in the temperature-density relation that is expected from the complex physics of the IGM and seen in cosmological hydrodynamic simulations. Persistence of gravitationally induced higher order correlations in the spectra requires that the scatter be no more than twice as large as already seen in hydrodynamic simulations of structure formation. This limits the role of “ad-

ditional” sources of fluctuations such as an inhomogeneous UV background field or radiative transfer effects. To further strengthen the case requires this correlation to be computed from more high-S/N, high-resolution quasar spectra such as that which could be obtained with Keck, Magellan, or similar telescopes. We hope that when more high-quality spectra along different lines of sight become available, this method will be a powerful tool to study any “extra” physical process, beyond gravity, in the IGM.

T. Fang thanks Rupert Croft, Patrick McDonald, Ravi Sheth, and Matias Zaldarriaga for helpful conversations. We thank M. Rauch and W. Sargent for providing Keck data of QSO 1422+231 and A. Meiksin for Keck data of HS 1946+7658. We also thank the referee for comments on our manuscript. T. Fang was supported by NASA through *Chandra* Postdoctoral Fellowship Award PF3-40030 issued by the *Chandra X-Ray Observatory* Center, which is operated by the Smithsonian Astrophysical Observatory for and on behalf of NASA under contract NAS8-39073. M. White was supported by the NSF and NASA. Parts of this work were done on the IBM-SP at the National Energy Research Scientific Computing Center.

## REFERENCES

- Bryan, G. L., Machacek, M., Anninos, P., & Norman, M. L. 1999, *ApJ*, 517, 13
- Cen, R., Miralda-Escudé, J., Ostriker, J. P., & Rauch, M. 1994, *ApJ*, 437, L9
- Croft, R. A. C., Weinberg, D. H., Bolte, M., Burles, S., Hernquist, L., Katz, N., Kirkman, D., & Tytler, D. 2002, *ApJ*, 581, 20
- Croft, R. A. C., Weinberg, D. H., Katz, N., & Hernquist, L. 1998, *ApJ*, 495, 44
- Hernquist, L., Katz, N., Weinberg, D. H., & Jordi, M. 1996, *ApJ*, 457, L51
- Hui, L., & Gnedin, N. Y. 1997, *MNRAS*, 292, 27
- Kirkman, D., & Tytler, D. 1997, *ApJ*, 484, 672
- Mandelbaum, R., McDonald, P., Seljak, U., & Cen, R. 2003, *MNRAS*, 344, 776
- McDonald, P., Miralda-Escudé, J., Rauch, M., Sargent, W. L. W., Barlow, T. A., Cen, R., & Ostriker, J. P. 2000, *ApJ*, 543, 1
- Meiksin, A., & White, M. 2003, *MNRAS*, 342, 1205
- . 2004, *MNRAS*, in press (astro-ph/0307289)
- Meiksin, A., White, M., & Peacock, J. A. 1999, *MNRAS*, 304, 851
- Rauch, M., Sargent, W. L. W., Barlow, T. A., & Carswell, R. F. 2001, *ApJ*, 562, 76
- Viel, M., Matarrese, S., Heavens, A., Haehnelt, M. G., Kim, T.-S., Springel, V., & Hernquist, L. 2004, *MNRAS*, 347, L26
- White, M. 1999, *MNRAS*, 310, 511
- Zaldarriaga, M., Seljak, U., & Hui, L. 2001, *ApJ*, 551, 48 (ZSH01)
- Zhang, Y., Anninos, P., & Norman, M. L. 1995, *ApJ*, 453, L57